ding paper, Phys. Rev. B 3, 4100 (1971).
[2]B. A. Loomis and O. N. Carlson, in *Reactive Metals*, edited by W. R. Clough (Interscience, New York, 1958), Vol. 2.
[3]Y. M. Smirnov and V. A. Finkel', Zh. Eksperim. i Teor. Fiz. 49, 1077 (1965) [Sov. Phys. JETP 22, 750 (1966)].
[4]H. Suzuki and S. Miyahara, J. Phys. Soc. Japan 21, 2735 (1966).
[5]V. A. Finkel', V. I. Glamazda, and G. P. Kovtun, Zh. Eksperim. i Teor. Fiz. 57, 1065 (1969) [Sov. Phys. JETP 30, 581 (1970)].
[6]W. Rostoker and A. S. Yamomoto, Trans. Amer. Soc. Metals 47, 1002 (1955).
[7]G. K. White and S. B. Woods, Phil. Trans. Roy. Soc. London A251, 273 (1959).
[8]J. P. Burger and M. A. Taylor, Phys. Rev. Letters 6, 185 (1961).
[9]H. Suzuki, S. Minomura, and S. Miyahara, J. Phys. Soc. Japan 21, 2089 (1966).
[10]D. I. Bolef, J. de Klerk, and G. B. Brandt, Bull. Am. Phys. Soc. 7, 236 (1962).
[11]H. Suzuki and S. Miyahara, J. Phys. Soc. Japan 20, 2102 (1965).
[12]A. R. Mackintosh and L. Sill, J. Phys. Chem. Solids 24, 501 (1963).
[13]L. E. Drain, Proc. Phys. Soc. (London) 83, 755 (1964).
[14]R. G. Barnes and T. P. Graham, Phys. Rev. Letters 8, 248 (1962).
[15]C. G. Shull and M. K. Wilkinson, Rev. Mod. Phys. 25, 100 (1953).
[16]D. G. Westlake, Phil. Mag. 16, 905 (1967).
[17]D. G. Westlake, Trans. AIME 239, 1341 (1967).
[18]R. E. Smith and D. I. Bolef, Phys. Rev. Letters 22, 183 (1969).
[19]See, for example, L. D. Landau and E. M. Lifshitz, *Statistical Physics* (Addison-Wesley, New York, 1958), p. 273ff.
[20]R. E. Smith, Ph.D. thesis (Washington University, St. Louis, Mo., 1969) (unpublished).
[21]G. A. Alers, Phys. Rev. 119, 1532 (1960).

PHYSICAL REVIEW B VOLUME 3, NUMBER 12 15 JUNE 1971

Lattice Vibrations of Thallium at 77 and 296 K*

T. G. Worlton†
Los Alamos Scientific Laboratory, Los Alamos, New Mexico 87544
and Idaho Nuclear Corporation, Idaho Falls, Idaho 83401
and
R. E. Schmunk
Idaho Nuclear Corporation, Idaho Falls, Idaho 83401
(Received 5 October 1970)

Lattice vibration frequencies of Tl at 77 and 296 K have been measured along the lines Δ and Σ by neutron inelastic scattering. Modified axially symmetric force-constant models were fitted to the neutron data and were used to calculate phonon-dispersion curves along other symmetry directions in the crystal. Frequency distributions calculated from the 77-K models are compared with the results of superconducting tunneling experiments of Clark and Dynes.

I. INTRODUCTION

Phonon-dispersion curves of a large number of hcp metals have been measured by neutron inelastic scattering, including Mg, [1,2] Be, [3,4] Zn, [5] Ho, [6] Y, [7] Zr, [8] Sc, [9] and Tb. [10] Many hcp metals undergo a transition to a bcc structure at high temperature. [11] Transition temperatures of hcp metals which undergo this transition and have been studied by neutron inelastic scattering are 1523 K for Be, 1715 K for Ho, 1760 K for Y, 1135 K for Zr, 1583 K for Tb, and 1608 K for Sc. [11] None of the neutron inelastic scattering studies report results above room temperature, so the hcp-bcc transition could be expected to have little effect on phonon modes studied previously.

The present paper reports a study of the lattice vibration frequencies of thallium along the directions [0001] and [01$\bar{1}$0] at 77 and 296 K. Since Tl undergoes the hcp-to-bcc transition at 507 K, a relatively low temperature, it was expected that considerable softening of modes which take part in the transition might be observed at room temperature.

Considerable study has been given to the mechanism for the bcc $\rightleftarrows$ hcp phase transformation. Habit-plane studies in Ti and Zr indicate that the transformation involves $\{112\}\langle 111\rangle$ shears in the bcc phase. Burgers[12] concluded that the $\{0001\}$ planes of the hcp phase of Zr become $\{110\}$ planes of the bcc phase. He showed that this could be accomplished by a primary shear along $\{10.0\}$ planes of the hcp phase in a $\langle 11.0\rangle$ direction. The reverse shear system in the bcc phase is $\{112\}\langle 111\rangle$ with small dilatation strains needed to complete the transformation in either direction. Fisher and Renkin[11] have pointed out that the $\{10.0\}\langle 11.0\rangle$ shear in the hcp phase corresponds to the C_{66} elastic shear modulus which displays a strong temperature

dependence in Ti and Zr relative to the shear modulus C_{44}. They suggest that the instability of the hcp structures in these metals relative to the bcc structures above the transformation temperatures results from the effects of the anharmonicity on the vibrational frequency spectrum of the hcp structure. In the case of Tl the temperature dependence of C_{66} relative to C_{44} is stronger than in either Ti or Zr, hence one would expect the anharmonicity of the C_{66} related modes to be greater still. It is hoped that neutron scattering studies such as this will contribute to the understanding of this transformation process.

The fact that thallium is a superconductor below 1.37 K provides another reason for interest in Tl lattice vibrations. Superconducting tunneling experiments on Tl have been performed by Clark[13] and by Dynes.[14] These experiments provide information about the frequency distribution in Tl at ~1 K which should be similar to the frequency distribution calculated from the models fitted to the 77-K neutron data. A comparison of the two indicates that there are some qualitative similarities and certain peaks can be identified, but there are some rather large differences. These differences are understandable since the superconducting tunneling experiments yield $\alpha^2(\omega)F(\omega)$ instead of $F(\omega)$, the temperatures are different, and the models available for fitting dispersion curves of hcp crystals are not entirely satisfactory. The frequency distribution at 77 K may be considerably different from the frequency distribution at 1 K because of the low Debye temperature (96 K),[15] so some of the differences in the two spectra are probably real.

A modified axially symmetric (MAS) model[16] with force constants out to the sixth nearest neighbors was used to fit the dispersion curves at both temperatures. One model at each temperature was required to fit the elastic constants in addition to the neutron data. A tensor force model was also fit to the 77-K data. Frequency distributions and dispersion curves for all symmetry points and lines were calculated for each model, but the curves will only be presented for one model at each temperature in the interest of brevity.

Herring's notation is used throughout the paper to label phonon branches.[17] Calculations of dispersion curves were made using the block diagonalized dynamical matrix for each symmetry direction as given by Warren[18] except for corrections along the lines R and P.[19] The elements of the dynamical matrix were defined as in the paper by DeWames *et al.*[16] and then transformed to agree with Warren's choice of coordinates.

II. EXPERIMENTAL DETAILS AND RESULTS

The thallium sample used in the experiment was a 6.6-cm^3 single crystal grown by the strain anneal technique at Materials Research Limited in England. The crystal was in the form of a right circular cylinder of 1.46 cm diam and 3.94 cm long with the hexagonal c axis at an angle of 53° to the cylinder axis.

All measurements were carried out on the triple axis spectrometer at the Materials Testing Reactor (MTR) in Idaho. The (0002) planes of a large Be crystal provided the incident monochromatic beam with a fixed energy of 54.6 meV. All phonons were measured by neutron energy loss (phonon creation) except for a few points measured by neutron energy gain as a check on the energy-loss data. The (111) planes of an Al crystal were used as the analyzer and the spectrometer was operated in the constant $\vec{q}$ mode with the W configuration.

The crystal had initially been set up at the HB-3 beam hole of the MTR using a double crystal monochromater consisting of two spherical Al crystals using the (111) scattering planes. Attempts to measure the dispersion curves of Tl at room temperature were unsuccessful with this experimental setup due to the low monochromatic flux available at the sample position. Later, the spectrometer was moved to the HT-1 south beam hole where the fast neutron flux was lower, making it feasible to change to the single Be monochromater. The Tl sample was then mounted in a cryostat and cooled to liquid-nitrogen temperature.

After making these improvements, phonons were observed at 77 K without too much difficulty except for the low-frequency and low-$\vec{q}$ modes. Table I lists the 77-K data along with the errors used in the least-squares fitting. Errors were assigned according to the quality of the data and are probably overestimated as indicated by the very low values of χ^2 obtained from the least-squares-fitting program. One further improvement was made in the experimental setup before attempting to measure the dispersion curves at room temperature. A Cu crystal, whose reflectivity had been optimized by a bending and straightening process, was mounted in the analyzer position using the (002) planes. Measurements of the room-temperature dispersion curves were then carried out using the 77-K data as a guide.

Table II displays the data obtained at room temperature together with the estimated errors which were used in the least-squares fitting. Again the data were quite good except for the low-frequency and low $\vec{q}$ modes. The transverse optical phonon at Γ_5^+ was especially troublesome because it was biased by an extremely high background. Measurements of the transverse optical phonons along Δ gave very poor results as evidenced by the scatter in the data for this branch. There was a large sloping background for all positions in the recip-

TABLE I. Thallium dispersion relation data at 77 K. Phonon energies ΔE and their respective errors $\Delta(\Delta E)$ are quoted in meV.

Mode	q/q_m	ΔE	$\Delta(\Delta E)$
$\Sigma_1 A$	0.2	•••	•••
	0.4	4.99	0.8
	0.6	6.95	0.4
	0.8	8.58	0.5
	1.0	8.95	0.5
$\Sigma_1 0$	0.0	5.3	1.5
	0.2	5.7	1.5
	0.4	6.74	0.4
	0.6	8.25	0.3
	0.8	9.3	0.3
	1.0	9.60	0.3
$\Sigma_3 A$	0.2	•••	•••
	0.4	2.35	0.5
	0.6	3.5	0.3
	0.8	4.2	0.3
	1.0	4.25	0.4
$\Sigma_3 0$	0.0	11.75	0.5
	0.2	11.68	0.3
	0.4	11.42	0.3
	0.6	11.04	0.3
	0.8	10.55	0.5
	1.0	9.95	0.5
$\Sigma_4 A$	0.2	•••	•••
	0.4	1.7	0.8
	0.6	2.7	0.6
	0.8	3.7	0.5
	1.0	4.0	0.6
$\Sigma_4 0$	0.2	5.3	1.5
	0.4	5.4	1.5
	0.6	5.75	0.5
	0.8	6.21	0.4
	1.0	6.52	0.3
$\Delta_1 A$	0.2	•••	•••
	0.4	3.3	0.5
	0.6	4.95	0.6
	0.8	6.2	0.5
	1.0	7.6	0.4
$\Delta_2 0$	0.2	11.5	0.3
	0.4	10.8	0.3
	0.6	9.4	0.7
	0.8	8.42	0.4
	1.0	7.6	0.4
$\Delta_6 A$	0.2	•••	
	0.4	1.25	0.4
	0.6	1.87	0.5
	0.8	2.40	0.9
	1.0	3.15	0.6
$\Delta_5 0$	0.2	4.65	0.9
	0.4	4.60	0.9
	0.6	4.00	0.5
	0.8	3.50	0.4
	1.0	3.15	0.6

TABLE II. Thallium dispersion relation data at 296 K. Phonon energies ΔE and their respective errors $\Delta(\Delta E)$ are quoted in meV.

Mode	q/q_m	ΔE	$\Delta(\Delta E)$
$\Sigma_1 A$	0.2	•••	•••
	0.4	4.95	0.8
	0.6	6.85	1.0
	0.8	8.75	0.9
	1.0	9.05	0.8
$\Sigma_1 0$	0.0	4.4	1.5
	0.2	5.5	1.5
	0.4	6.6	1.5
	0.6	8.2	0.6
	0.8	9.35	0.8
	1.0	9.65	0.7
$\Sigma_3 A$	0.2	•••	•••
	0.4	2.45	0.7
	0.6	3.2	0.4
	0.8	4.3	0.4
	1.0	5.0	0.6
$\Sigma_3 0$	0.0	11.60	0.5
	0.2	11.5	0.7
	0.4	10.35	0.6
	0.6	8.95	0.9
	0.8	7.90	0.8
	1.0	7.00	1.0
$\Sigma_4 A$	0.2	•••	•••
	0.4	1.32	0.5
	0.6	2.50	1.0
	0.8	3.20	0.5
	1.0	3.35	0.3
$\Sigma_4 0$	0.2	4.50	1.50
	0.4	4.65	1.50
	0.6	4.80	0.50
	0.8	5.50	0.50
	1.0	5.80	0.40
$\Delta_1 A$	0.2	•••	•••
	0.4	3.00	1.00
	0.6	4.60	0.70
	0.8	5.65	0.50
	1.0	6.95	0.50
$\Delta_2 0$	0.2	11.25	0.90
	0.4	10.80	0.90
	0.6	9.65	1.20
	0.8	7.80	1.00
	1.0	6.95	0.50
$\Delta_6 A$	0.2	•••	•••
	0.4	•••	•••
	0.6	2.0	0.50
	0.8	2.52	0.60
	1.0	2.85	0.50
$\Delta_5 0$	0.2	2.65	1.50
	0.4	2.85	0.80
	0.6	2.92	1.00
	0.8	3.05	0.60
	1.0	2.85	0.50

rocal lattice with small wave vector which arose from elastic scattering. At $\tilde{q} = 0$ the background was evident even in the highest frequency optical mode.

A typical phonon at the two temperatures is displayed in Fig. 1. This is the phonon observed where the Δ_1 and Δ_2 branches meet at A_1 on the zone boundary. It was impossible to determine whether the neutron data were in agreement with the elastic constants because of inadequate resolution at the low frequencies. The sample crystal had a mosaic spread of about 30′ which, combined with the high ratio of sample temperature to Debye temperature and the high incident energy, resulted in relatively broad phonon peaks. Collimation between the monochromater and sample was 0.5°, while between sample and analyzer it was 0.6°. The use of finer collimation was tried with no noticeable improvement in resolution. Recently developed highly oriented graphite monochromaters can be used to improve both intensity and resolution in measurements of low-frequency modes[20] and presumably could be used to obtain much improved data on the low-frequency modes of Tl. Unfortunately, the MTR has been shut down and the present authors can make no further measurements.

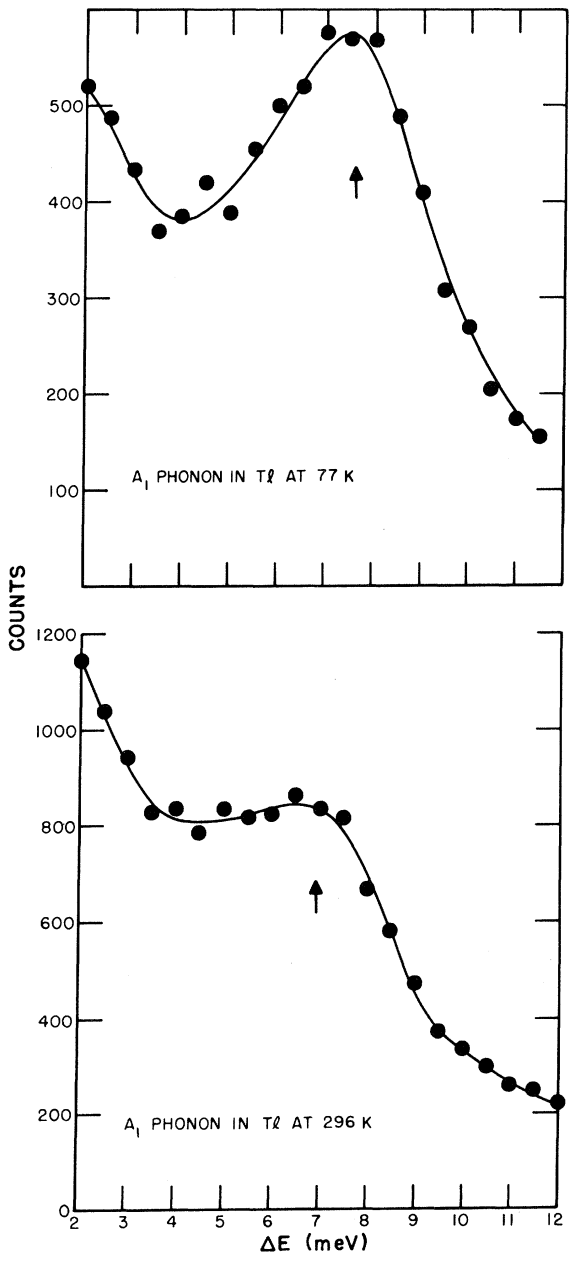

FIG. 1. Typical neutron group showing raw data obtained for the A_1 mode in Tl at 77 and 296 K. The arrow indicates the peak position determined after subtracting background. The solid curves are merely a guide for the eye.

III. DISCUSSION

In the tensor force model for a hcp crystal there are four independent force constants per neighbor for interactions with first, second, and third nearest neighbors and two independent constants for interactions with fourth nearest neighbors.[21] The axially symmetric (AS) model reduces the number of independent force constants per neighbor to two by requiring that the components of the bond bending force along the x and z directions be equal. Another model which has been used for hcp crystals is the Slutsky-Garland (SG) model[22] which is obtained from the AS model by setting the bond bending force constants equal to zero. DeWames *et al.* were unable to obtain good elastic agreement in Be, β-Sn, and Zn using the AS and SG models, so they introduced the MAS model in which the x and z components of the bond bending force constants are required to be proportional with the same constant of proportionality σ_B for all sets of neighbors.[16] This model is generally defined out to sixth neighbors and thus has 13 adjustable parameters as compared with 11 for the fourth-neighbor TF model (only 11 of the 14 force constants in the TF model apply along the symmetry directions of interest). Other models with a smaller number of parameters have been discussed recently by Metzbower[23] and by Sharan and Bajpai.[24] These models appear to be successful in reducing the number of parameters, but not in improving the fit to all the data. Since none of the models appear to have too much physical significance, it was decided to use the MAS model to fit the Tl data since a computer program for calculating frequency distributions from this model was readily available.[25]

After obtaining a least-squares fit to the data along the Δ and Σ directions, the force-constant models were used to calculate the dispersion curves along the T, R, S, U, and P directions. A separate calculation was made at the point M to determine the ordering of the modes since they cannot be uniquely determined from compatibility relations, but it was found that the symmetry labels were

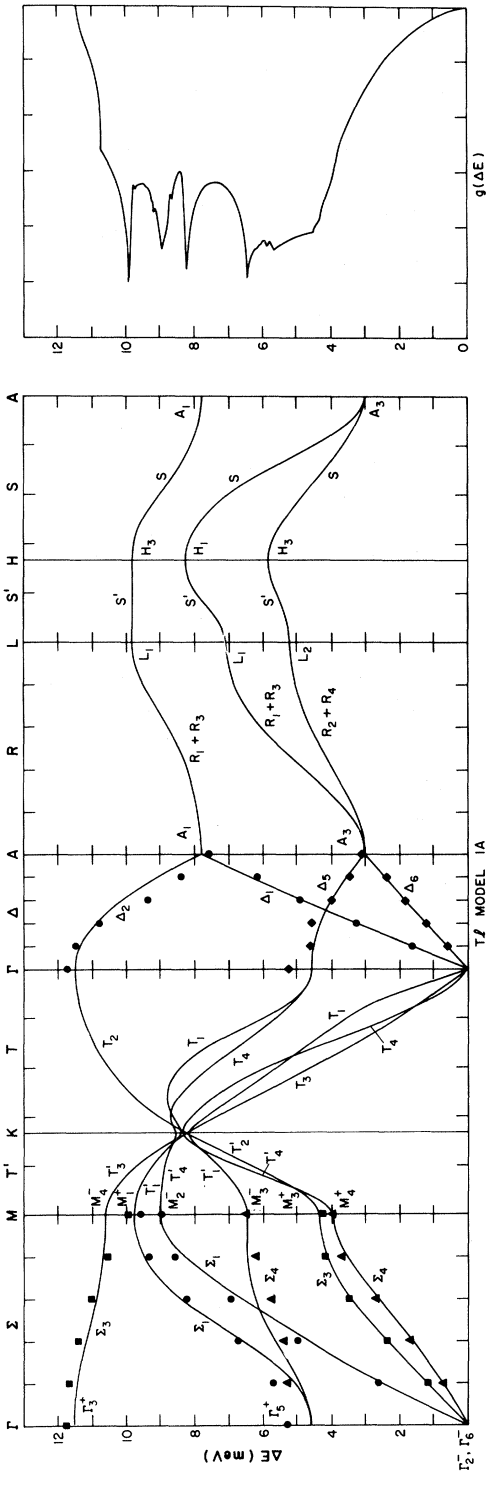

FIG. 2. Phonon-dispersion curves of Tl at 77 K plus phonon frequency distribution calculated from model 1*A*. Solid circles represent data points for longitudinal modes while other data points are for transverse modes. The data points at $\frac{1}{5}$ of the way to the zone boundary for the acoustic branches are calculated from the elastic constants.

still ambiguous because different models gave different identification of the modes. Frequencies were calculated for the extra symmetry directions in order to identify some of the peaks in the frequency distribution and to see if there appear to be any exceptionally low-frequency modes on the zone boundary at room temperature. Figure 2 shows the dispersion curves calculated from model 1*A* plus the frequency distribution calculated from this model together with the 77-K neutron data. Points at $q = 0.2q_{\max}$ on the acoustic branches were obtained from the elastic constants since these modes could not be determined accurately from the neutron data. Parameters of the models obtained from least-squares fitting to the 77-K data are presented in Table III. Models 1*A* and 2*A* are MAS models which differ only in that 1*A* (2*A*) was (not) required to simultaneously fit the elastic constants, and TF is a tensor force model. For the MAS models only the x components of the bond bending force constants are given since the z components can be obtained by multiplying by σ_B. Relations between the force constants given here for the tensor force model and those usually used are given by DeWames *et al.*[16] Parameters α_4 and β_{4z} of the TF model occur in the elements of the dynamical matrix only as a sum so they cannot be evaluated independently.

Elastic constants calculated from the three 77-K models are presented in Table IV together with the experimental elastic constants measured by Ferris and co-workers[26] after correcting for the small temperature difference. Also included in the table is the dimensionless parameter χ^2 which indicates the quality of the fit of each model to the data. χ^2 is determined from the equation

$$\chi^2 = [\sum (\nu_T^2 - \nu_E^2)^2]^{1/2} / 2\nu_E \, \Delta\nu_E (N - M) \ , \qquad (1)$$

where N is the number of frequencies measured, M is the number of free parameters in the model, ν_T is the frequency calculated from the model, ν_E is the experimental frequency, and $\Delta\nu_E$ is the error assigned to the experimentally measured frequency. In model 1*A* the elastic constants are essentially exact because the elastic constants were included as data with small error in the least-squares fitting. However, DeWames *et al.* give two independent equations for determining the elastic constant C_{44}, the two equations resulting from considering waves propagating in the basal plane and along the c axis. The relation

$$C_{44} = (4\gamma^2/c\sqrt{3})(\tfrac{3}{2}\delta_1 + 6\delta_3 + 21\delta_5 + \beta_{4x} + \tfrac{3}{4}\epsilon_{1x} + \tfrac{3}{4}\epsilon_{3x} + \tfrac{3}{2}\epsilon_{5x}) \qquad (2)$$

was used to determine the value of C_{44} in the least-squares fitting. A value for C_{44} was also calculated using the relation

TABLE III. Parameter values obtained for the modified axially symmetric (MAS) (1A and 2A) and tensor force (TF) lattice dynamics models by a least-squares fitting to the thallium dispersion relation data for 77 K. Models 1A and 2A differ in the errors assigned to the elastic constants which were included in the fitting routine. With the exception of σ_B which is dimensionless, the force constants are in units of dyn cm^{-1}. $\delta_1 = K_1/(4+3\gamma^2)$, $\delta_3 = K_3/(16+3\gamma^2)$, $\delta_5 = K_5/(28+3\gamma^2)$.

	Model 1A	Model 2A	TF	
K_1	10247.5	10734.7	12115.1	
ϵ_{1x}; ϵ_{1z}	−1927.8	−1714.1	−834.9;	2483.0
α_2	10540.6	10628.3	11529.9	
β_{2x}, β_{2z}	−73.3	−155.8	−1174.1;	321.3
K_3	−2386.0	−2446.9	−3045.1	
ϵ_{3x}, ϵ_{3z}	860.3	876.0	1101.9;	−1164.2
α_4	−1488.7	−1659.1	−906.4	
β_{4x}	−252.7	−223.0	−195.9	
K_5	1816.2	1467.4	...	
ϵ_{5x}	31.4	7.9	...	
α_6	−1159.9	−999.7	...	
β_{6x}	100.8	74.4	...	
σ_B	−1.91267	−2.03625	...	

$$C_{44} = (4/c\sqrt{3})(\tfrac{3}{2}\gamma^2\delta_1 + 6\gamma^2\delta_3 + 21\gamma^2\delta_5 + \tfrac{3}{2}\beta_{2z} + \tfrac{9}{2}\beta_{6z} + \tfrac{1}{2}\epsilon_{1z} + 2\epsilon_{3z} + 7\epsilon_{5z}) \quad , (3)$$

and this is listed following the C_{44} calculated from Eq. (2) in Tables IV and VI.

Since C_{13} is given in terms of C_{44} by the equation

$$C_{13} = -C_{44} + (4\gamma^2/c\sqrt{3})(3\delta_1 + 12\delta_3 + 42\delta_5) \quad , \qquad (4)$$

there are also two independent equations for C_{13}. Agreement between the values obtained from the two cases is good to a few percent in models 1A and 2A, but the two sets of values are significantly different for the TF model. Model 2A fits the elastic constants within about 5% except for C_{13} which differs by 12%. The tensor force model gave a much poorer fit to the elastic constants, especially C_{13}.

Figure 3 shows calculations from model 1B plus the 296-K neutron data. Figures 4 and 5 show dispersion curves along additional symmetry directions calculated from models 1A and 1B. A comparison of Figs. 2 and 3 indicates a considerable change in the mode frequencies at points L and H as a function of temperature. These may be meaningless, however, because the models have been obtained from fitting data along the Δ and Σ directions only. Most neutron inelastic scattering experiments have been confined to these symmetry directions but McDonald *et al.*[5] have recently extended the measurements of the dispersion curves of zinc to the T direction. They found that previous MAS models which gave a good fit to the neutron data along Δ and Σ gave a poor fit to their data along T. They also attempted to fit their data with a two-parameter model pseudopotential with very poor success. This indicates that a great deal of work needs to be done yet on the theory of the lattice dynamics of hcp metals.

Table V gives the parameters of the two MAS models fitted to the room-temperature data and Table VI gives the elastic constants and fitting parameters for these models together with the experimental values of the elastic constants as obtained from Ref. 26.

Model 1B was fitted to both the neutron data and the experimental elastic constants using Eqs. (2) and (4) to calculate C_{44} and C_{13}. The value of C_{44} calculated using the parameters from the fitting in Eq. (3) was off by almost 6%. Elastic constants calculated from model 2B are not satisfactory. The calculated value of C_{33} is off by 10%, while C_{44} and C_{13} are off by 20% and 49% if Eq. (2) is used to calculate C_{44}. If Eq. (3) is used to calculate C_{44}, it is in error by less than 2%, but C_{13} is still off by 42%. Thus it would appear that model 1B is the preferable model for the room-temperature data. It was also possible to fit the room-temperature data with MAS models having a negative value of σ_B as in the 77-K case, but these are not presented here because the fitting parameter χ^2 was larger for these models. It was not possible to fit the 77-K data with a MAS model having a positive value of σ_B. When this was attempted the least-squares-fitting routine either oscillated back and forth between two secondary minima or converged to a set of parameters with a negative σ_B.

It is felt that the force constants of the models presented here have no physical significance but are useful in providing a representation of the data and in calculating frequency distributions and dispersion curves for other symmetry directions.

Sharan and Bajpai have recently developed a model for the lattice dynamics of hexagonal-close-

TABLE IV. Elastic constants (in units of 10^{12} dyn cm^{-2}) for 77 K calculated from the relations between elastic constants and force constants for the parameter values and different models given in Table III. The experimental data of Ferris *et al.* (Ref. 26) are included for comparison. The parameter χ^2 indicates the quality of fit between the various models and the experimental data.

	Model 1A	Model 2A	TF	Expt
C_{11}	0.4346	0.4069	0.3456	0.4346
C_{12}	0.3697	0.3526	0.2964	0.3697
C_{13}	0.2992; 0.2976[a]	0.2643; 0.2644[a]	0.0840; 0.1100[a]	0.2992
C_{33}	0.5880	0.5586	0.5688	0.5880
C_{44}	0.0835; 0.0850[a]	0.0844; 0.0843[a]	0.0850; 0.0590[a]	0.0835
χ^2	0.31334[b]	0.30706	0.48238	

[a]Values corresponding to second definition of C_{44} in Ref. 16.

[b]Elastic constants included in fitting.

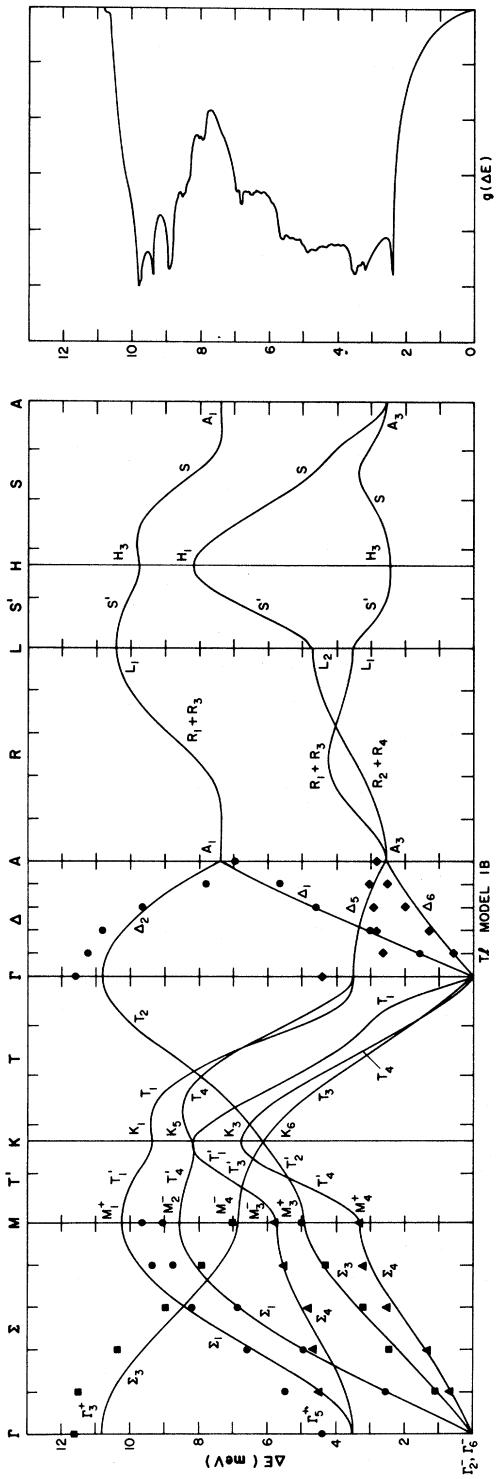

FIG. 3. Phonon-dispersion curves of Tl at 296 K plus the phonon frequency distribution calculated from model 1*B*. Solid circles represent longitudinal modes and other points represent transverse modes. For the acoustic branches the data points at $\frac{1}{6}$ of the way to the zone boundary are calculated from the elastic constants. Data on the Δ_5 optic mode were very poor.

packed metals which takes the electron-ion contribution to the lattice dynamics into account explicitly.[24] They have applied their model to beryllium, magnesium, and thallium. Dispersion curves calculated using only five parameters show excellent agreement with experiment for Be and Mg.[24] Curves calculated for Tl using the 4.2-K elastic constants are in poor agreement with the results reported here, but this may be due to an error in their calculations. The initial slope of the longitudinal acoustic branch in the Δ direction shown in Fig. 3 of Ref. 24 is in serious disagreement with the initial slope calculated from the relation $\rho\omega^2 = C_{33}q^2$.[16] This seems strange since their force constants were determined from the elastic constants. The transverse branches which they report for the Δ direction are in fairly good agreement with the results reported in the present study. For the Σ direction they show the Σ_1 acoustical and Σ_4 optical branches not crossing, which is in disagreement with our data. Their calculation also has the Γ_3^+ optical mode about 20% lower than the value determined here.

Clark[13] and Dynes[14] have performed superconducting tunneling experiments on Tl at ~1 K. These experiments can be used to obtain $\alpha^2(\omega)F(\omega)$,[14] where $\alpha^2(\omega)$ is a measure of the electron-phonon

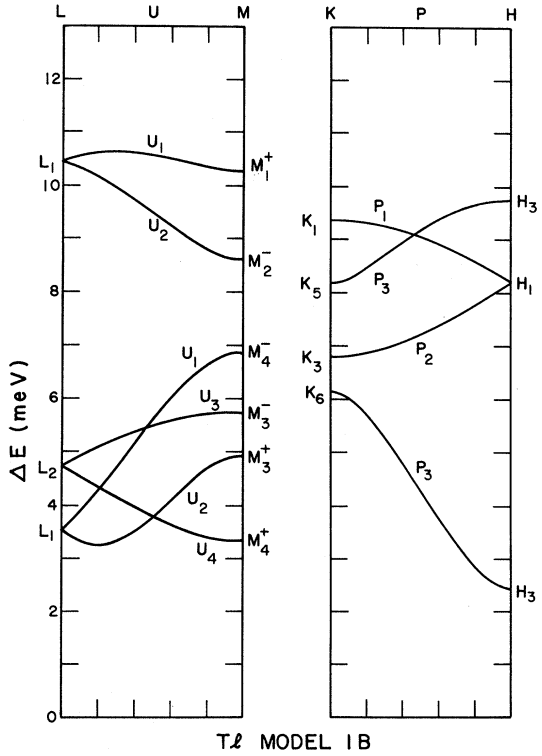

FIG. 4. Dispersion curves of Tl at 77 K along the directions *U* and *P* as calculated from model 1*A*.

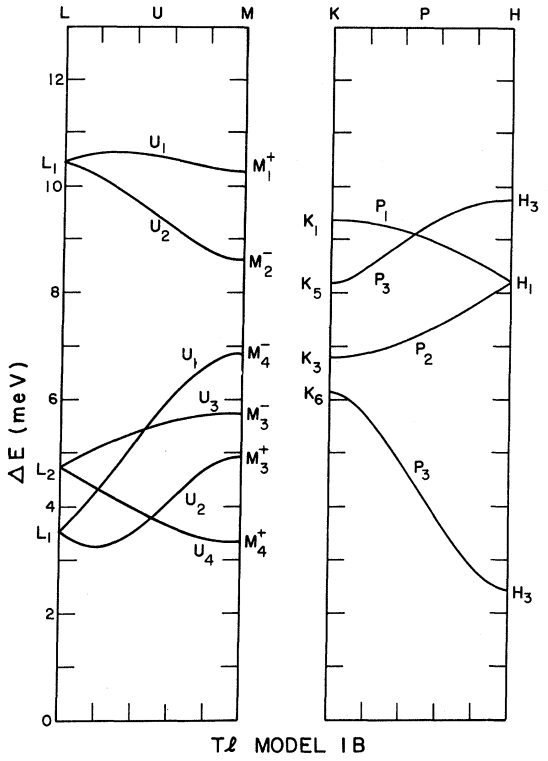

FIG. 5. Dispersion curves of Tl at 296 K along the directions U and P as calculated from model 1B.

interaction and $F(\omega)$ is the phonon density of states. The electron-phonon interaction is thought to be slowly varying so that $\alpha^2(\omega)F(\omega)$ can be compared directly with the frequency distribution. [14] Clark reported the end of the phonon spectrum at 10.6 meV but saw a strong end point singularity at

TABLE V. Parameter values obtained by least-squares fitting the modified axially symmetric (MAS) model to the thallium dispersion relation data at 296 K with (1B) and without (2B) requiring the parameters to simultaneously fit the elastic constants. Values are quoted in units of dyn cm^{-1}. $\delta_1 = K_1/(4+3\gamma^2)$, $\delta_3 = K_3/(16+3\gamma^2)$, $\delta_5 = K_5/(28+3\gamma^2)$.

	Model 1B	Model 2B
K_1	15 491.1	14 484.8
ϵ_{1x}	−2 421.6	−2 169.8
α_2	12 870.4	13 081.3
β_{2x}	−1 157.1	−1 716.2
K_3	−481.9	−1 524.2
ϵ_{3x}	608.8	883.9
α_4	−884.6	−1 823.9
β_{4x}	78.5	316.9
K_5	−295.5	−610.0
ϵ_{5x}	177.4	251.4
α_6	−321.2	334.8
β_{6x}	−274.8	−194.8
σ_B	1.56194	1.13335

TABLE VI. Elastic constants (in units of 10^{12} dyn cm^{-2}) for 296 K calculated using the force-constant values quoted in Table V and compared to the experimental data of Ferris *et al.* (Ref. 26). The parameter χ^2 indicates the quality of fit between the various models and the experimental data.

	Model 1B	Model 2B	Expt
C_{11}	0.4083	0.4099	0.4083
C_{12}	0.3541	0.3508	0.3540
C_{13}	0.2896; 0.2936[a]	0.1482; 0.1671[a]	0.2896
C_{33}	0.5291	0.4745	0.5291
C_{44}	0.0727; 0.0686[a]	0.0904; 0.0715[a]	0.0727
χ_2	0.51993[b]	0.45510	

[a]Values corresponding to second definition of C_{44} in Ref. 16.

[b]Includes fitting to elastic constants.

11.2 meV in curves of d^2I/dV^2 against V. [13] Dynes found that $\alpha^2(\omega)F(\omega)$ went to zero at $\hbar\omega = 11.2$ meV.[14] The end of the spectrum at 77 K determined from the present experiment is $\hbar\omega = 11.75$ meV. Clark also reported peaks at 4.0 and 9.45 meV. [13] Dynes reported strong peaks at 3.9 and 9.5 meV, [14] in good agreement with Clark. The frequency distribution calculated from model 1A for 77 K does not display a peak at 4.0 meV even though the Σ_4 acoustical branch approaches the zone boundary with this limiting value. This could be due to a temperature effect as evidenced by the shifting of both Σ_3 and Σ_4 acoustical branches from 296 to 77 K, or it may be due to deficiencies in the model.

The peak which Clark and Dynes report at ~ 9.5 meV almost surely corresponds to the longitudinal modes at M. Our measurements show the longitudinal optical Σ_1 branch meets M at 9.6 meV, while the Σ_1 acoustical branch comes in at 8.95 meV. Dynes reports additional smaller peaks at about 6.1 and 7.5 meV. [14] Clark reports a number of different peaks[13] but it is difficult to determine from his discussion which peaks may actually correspond to peaks in the frequency spectrum. Figure 2 shows strong peaks in the frequency distribution calculated from model 1A at 9.9, 8.9, 8.0, and 6.4 meV. There is a distinct shoulder at 4 meV due to the Σ_3 and Σ_4 acoustical modes. In general it appears that the critical points in the frequency distribution calculated from the neutron data occur at higher frequencies than the corresponding points determined from superconducting tunneling. This could be a real difference due to actual differences in the frequency distributions at 1 and 77 K or to variations in $\alpha^2(\omega)$. On the other hand the MAS models used in fitting the neutron data along Δ and Σ are known[5] to give poor results along T in the case of zinc and may not produce an accurate frequency distribution. This indicates

that further neutron inelastic scattering measurements are needed in order to obtain a more accurate model for calculating frequency distributions.

ACKNOWLEDGMENT

The authors would like to thank Professor R. J. Kearney of the University of Idaho, who provided the Tl crystal used in this experiment.

*Work supported by the U. S. Atomic Energy Commission.

†Present address: Solid State Science Division, Argonne National Laboratory, Argonne, Ill. 60439.

[1]P. K. Iyengar, G. Venkataraman, P. R. Vijayaraghavan, and A. P. Roy, in *Inelastic Scattering of Neutrons in Solids and Liquids* (International Atomic Energy Agency, Vienna, 1965), Vol. I, p. 153.

[2]G. L. Squires, Proc. Phys. Soc. (London) 88, 919 (1966); G. L. Squires and R. Pynn, in *Neutron Inelastic Scattering* (International Atomic Energy Agency, Vienna, 1968), Vol. I, p. 215.

[3]R. E. Schmunk, R. M. Brugger, P. D. Randolph, and K. A. Strong, Phys. Rev. 128, 562 (1962).

[4]R. E. Schmunk, Phys. Rev. 149, 450 (1966).

[5]D. L. McDonald, M. M. Elcombe, and A. W. Pryor, J. Phys. C 2, 1857 (1969). Additional references on zinc are given in this article.

[6]J. A. Leake, V. J. Minkiewicz, and G. Shirane, Solid State Commun. 7, 535 (1969).

[7]S. K. Sinha, T. O. Brun, L. D. Muhlestein, and J. Sakurai, Phys. Rev. B 1, 2430 (1970).

[8]H. F. Bezdek, R. E. Schmunk, and Leonard Finegold, Phys. Status Solidi 42, 275 (1970).

[9]N. Wakabayashi and S. K. Sinha, Phys. Rev. B (to be published).

[10]J. C. Glyden Houmann and R. M. Nicklow, Acta Cryst. A25, Part S3, S253 (1969).

[11]E. S. Fisher and C. J. Renkin, Phys. Rev. 135, A482 (1964).

[12]W. G. Burgers, Physica 1, 561 (1934).

[13]T. D. Clark, J. Phys. C 1, 732 (1968).

[14]R. C. Dynes, Phys. Rev. B 2, 644 (1970).

[15]*International Tables for X-Ray Crystallography*, Vol. III (Kynoch Press, Birmingham, England, 1962).

[16]R. E. DeWames, T. Wolfram, and G. W. Lehman, Phys. Rev. 138, A717 (1965).

[17]C. Herring, J. Franklin Inst. 233, 525 (1942).

[18]J. L. Warren, Rev. Mod. Phys. 40, 38 (1968).

[19]Equations 6.151 of Ref. 18 are incorrect because 6.149 omits the $D_{yz}(12)$-type elements. There should also be an equation following (6.144) in Ref. 18 which reads $\omega_2(k_{10}) = A + iC - 2\omega^2 dD$.

[20]T. Riste and K. Otnes, Nucl. Instr. Methods 75, 197 (1969).

[21]M. F. Collins, Proc. Phys. Soc. (London) 80, 362 (1962).

[22]L. J. Slutsky and C. S. Garland, J. Chem. Phys. 26, 787 (1957).

[23]E. A. Metzbower, Phys. Rev. 177, 1139 (1969).

[24]B. Sharan and R. P. Bajpai, J. Phys. Soc. Japan 28, 338 (1970).

[25]L. J. Raubenheimer and G. Gilat, OR GHX South African Atomic Energy Board Report No. PEL 178, 1968 (unpublished).

[26]R. W. Ferris, M. L. Shepard, and J. F. Smith, J. Appl. Phys. 34, 768 (1963).